Divertor physics

P. Innocente[(1)], S. Roccella [(2)], L. Balbinot[(3)], G. Aberti[(4)] ….

on behalf of DTT Plasma Edge group, In-Vessel Component Team

[(1)]Consorzio RFX , [(2)]ENEA, [(3)]Università della Tuscia , [(4)]Politecnico di Milano

EUROfusion Science Meeting

12th June 2024

Power exhaust parameters

$q \propto P_{SOL}$

$A \propto 1/R$

$\lambda \propto B^{0.77}$

	AUG	JET	DTT	JT60-SA	ITER	DEMO
R (m)	1.65	3.0	2.19	2.96	6.2	9
a(m)	0.5	1.0	0.69	1.18	2.0	2.9
Ip (MA)	1.6	4	5.5	5.5	15	19.5
B_T (T)	3.1	3.45	5.85	2.25	5.3	5.7
Vp (m^3)	13	80	28	131	853	2218
<n> (10^{20} m^{-3})	1	1	1.8	0.6/0.9	1.0	0.8
P_{Tot} (MW)	27	40	45	41	150	450
P_{SOL} (MW)	**22**	**30**	**33**	**30**	**120**	**150**
P_{SOL}/R (MW/m)	**13**	**10**	**15**	**10**	**19.3**	**17**
P_{SOL}B/R (MW*T/m)	**40**	**34**	**88**	**23**	**102**	**99**
τ_E (s)	*	*	0.42	0.55/0.68	8.5	3.4
<T> (keV)	2	5	6.2	6.3	8.5	12.7
β_N	*	*	3.1	4.4	2.1	2.5
$\nu^*(10^{-2})$	*	*	1.8	4.1	2.4	2.2
$\rho^*(10^{-3})$	*	*	2.7	2.0	0.3	0.3

DTT power exhaust parameters are close to the ones of ITER and DEMO

DTT and DEMO ADCs

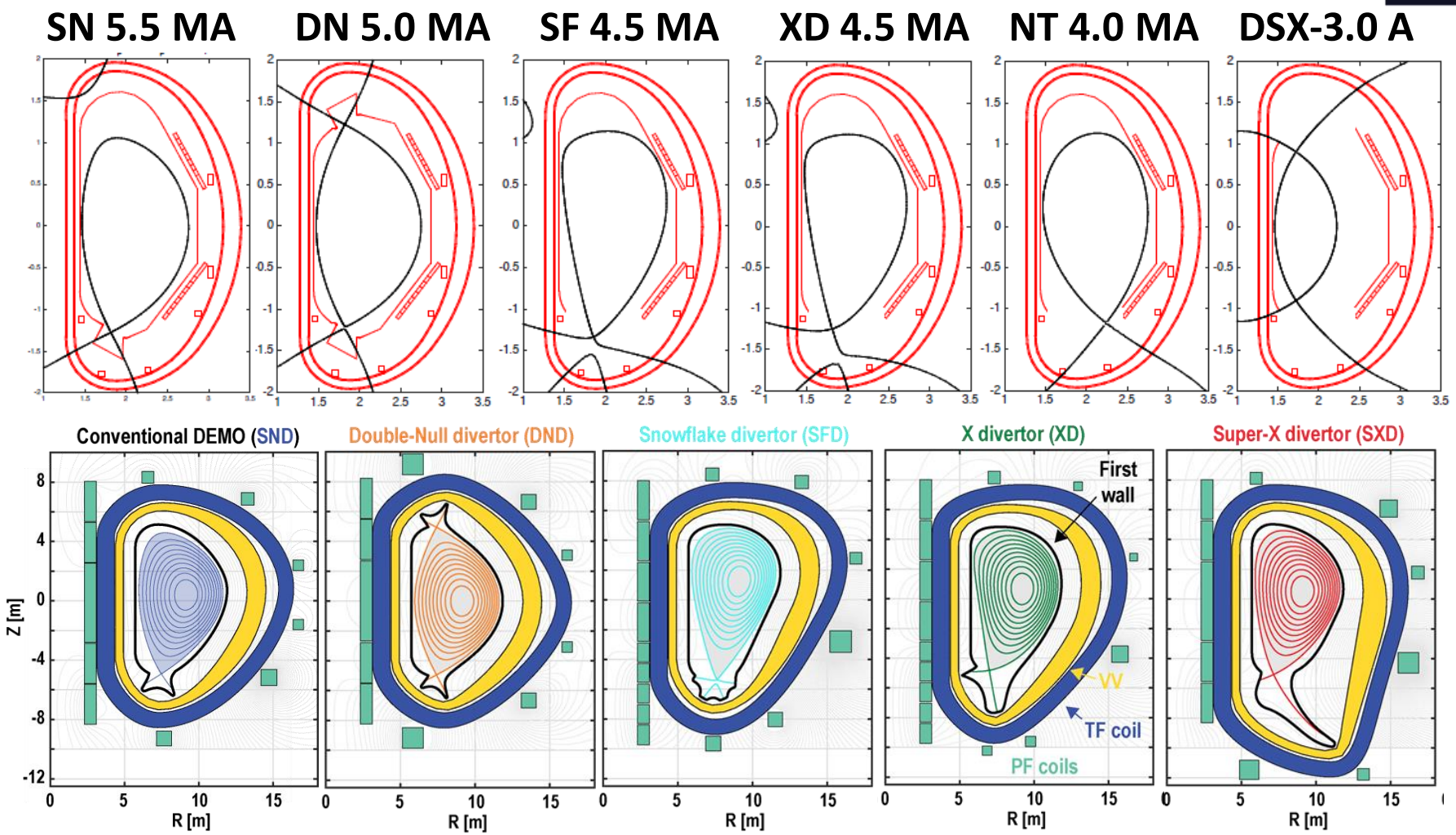

DTT magnetic system can realize all foreseen Alternative Divertor Configurations considered for DEMO

Divertor Requirements

- In a priority order, it must be compatible with following reference magnetic configurations: **SN-PT, XD and SN-NT**
- Reference configurations produced and **controlled with external coils only**
- **Forward B_t** for SN and XD, **reversed B_t** for NT
- **Counter-clockwise plasma current** in all reference scenarios but I-mode done in reversed B_t without NBI
- Flexible for experimental exploitation at plasma relevant parameters: **wide range in terms of X-point and strike points positions**
- Flexible in terms of low priority additional magnetic configurations: **long-leg SN and XD**
- SN-PT strike point **sweeping amplitude ≥ 14 cm**

Reference magnetic configurations

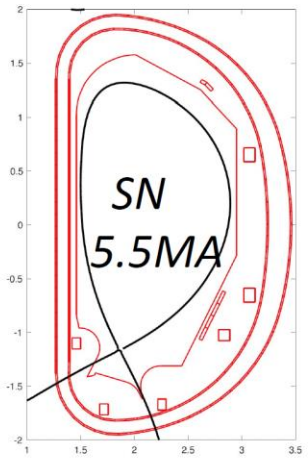

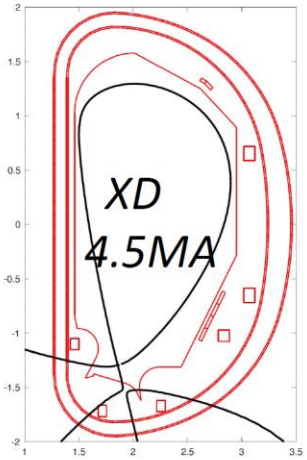

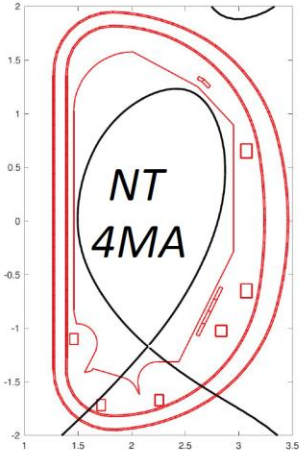

- Magnetic configurations can be realized at different maximum plasma current
- SN-PT can be produced up to 5.5 MA
- SN-PT and SN-NT have similar q_{95}
- SN-PT and XD have similar plasma volume
- SN-PT has high triangularity
- SN-NT has high negative upper triangularity (which seems to play the major role)

Plasma Configuration	SN	XD	NT
I_p [MA]	5.50	4.50	4.00
β_p	0.65	0.65	0.40
l_i	0.80	0.80	0.80
R_{axis} [m]	2.28	2.31	2.26
Z_{axis} [m]	0.19	0.30	0.23
$R_{X-point}$ [m]	1.86	1.87	2.15
$Z_{X-point}$ [m]	-1.16	-1.29	-1.17
R [m]	2.20	2.20	2.20
a [m]	0.70	0.70	0.69
$B_{tor,tot}$ at R_{axis} [T]	-5.96	-5.92	-5.82
$q_{95\%}$	-2.89	-3.66	-3.06
Elongation at sep. (k)	1.78	1.85	1.68
$k_{95\%}$	1.65	1.67	1.56
Triangularity at sep. (δ)	0.45	0.37	-0.15
$\delta_{95\%}$	0.33	0.25	-0.12
$\delta_{95\%,upper}$	0.37	0.24	-0.33
$\delta_{95\%,lower}$	0.29	0.25	0.08
Perimeter [m]	6.18	6.41	5.79
Volume [m^3]	34.19	34.39	30.97

The divertor

The Divertor consists of: **54** actively water-cooled **modules** (3 for each 20° sector) and supplied in parallel. **Water Cooling System**:

- inlet pressure: **5MPa**
- total mass flow rate up to: **577 kg/s**
- inlet temperature: **within 30-130°C**

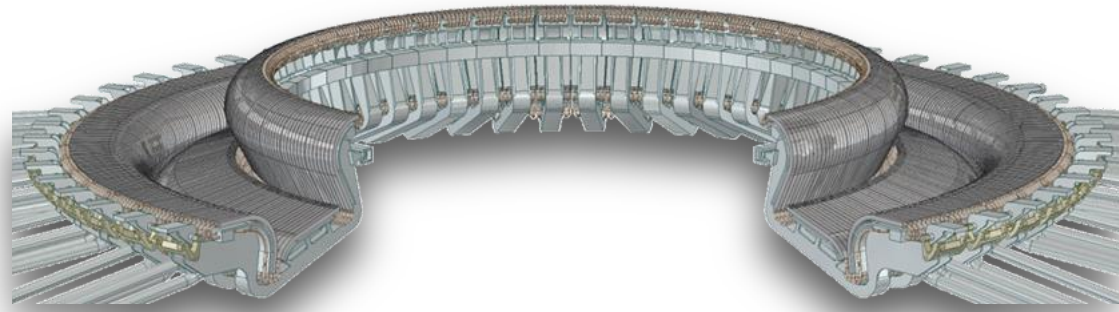

The **4 central cassettes** in the RH ports **are devoted to testing materials and technologies.** This central **cassettes have to be easily replaced (**without removing adjacent cassettes and piping) and can be supplied by **a dedicated water cooling system (43 kg/s; up to 250°C. up to 15 MPa)**

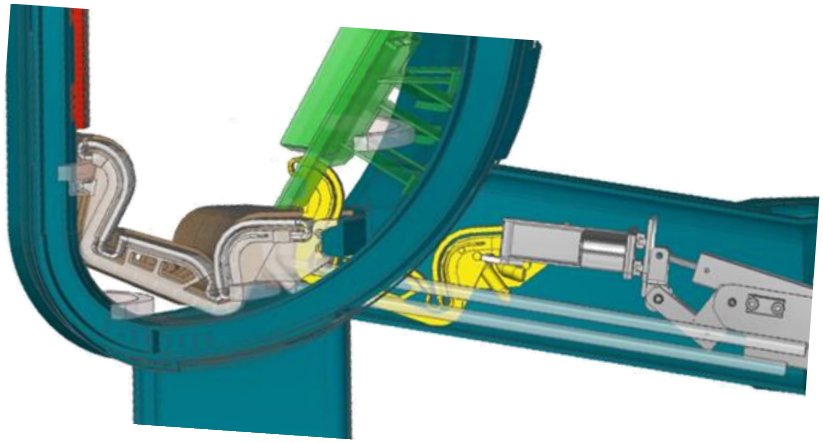

Target toroidal shaping

To maximize the allowable power on the targets ⟶ **Unidirectional**

OHT tilting is achieved by increasing the thickness of the armour

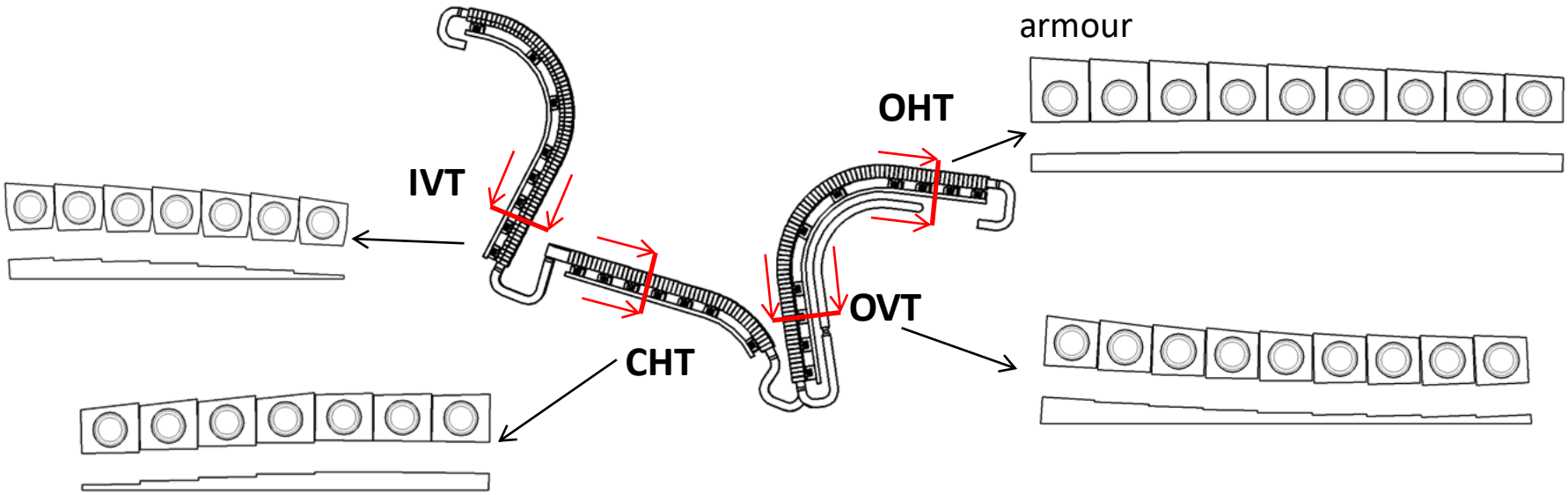

To allow compatibility with NT and XD only 4 PFUs are tilted

	α (°)	l_{mb} (mm)	g_{cas} (mm)	$Step_{cas}$ (mm)	g_{PFU} (mm)	$Step_{PFU}$ (mm)	θ_{bevel} (°)
IVT	2.3 (SN)	24.6	8	0±2	0.4÷0.5	0±0.3	1.6
OVT	2.2 (SN)	25	8	0±2	0.4÷0.5	0±0.3	1.4
CHT	3.6 (NT)	26	8	0±1.5	0.4÷0.5	0±0.2	1.7
OHT	1.4 (NT)	27	8	0±2	0.4÷0.5	0±0.3	1.2

Full power modeling for divertor design

- **Full power operation (P_{ADD}=45 MW)** with about 1/3 of the power dissipated in the core (based on core modeling)
- **Density controlled by gas-puffing and pumping** (negligible core particle flux from NBI 10 MW @ 510 keV)
- Power crossing separatrix higher than minimum requested for **H-mode operation** in positive triangularity (no X-point radiation configuration)

- ELMs not considered in modeling but average ELMs power (5 MW) subtracted from stationary heat flux
- **Transport in agreement with Eich scaling** in terms of heat flux decay length ($\lambda_q \cong 1$ mm) with radial **profiles as in present devices** (to get a better description up to top of pedestal)

Analysed configurations

Reference configurations

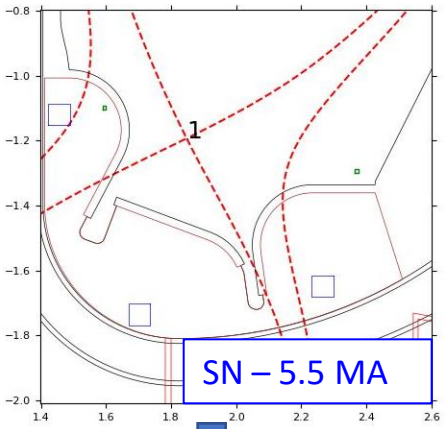

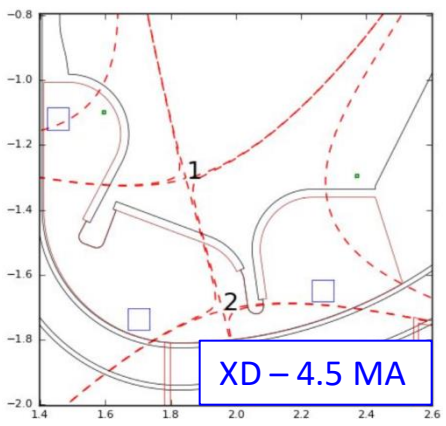

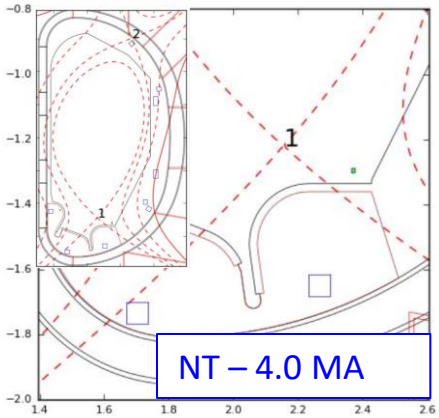

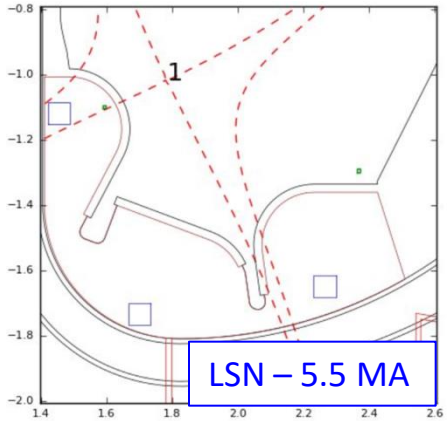

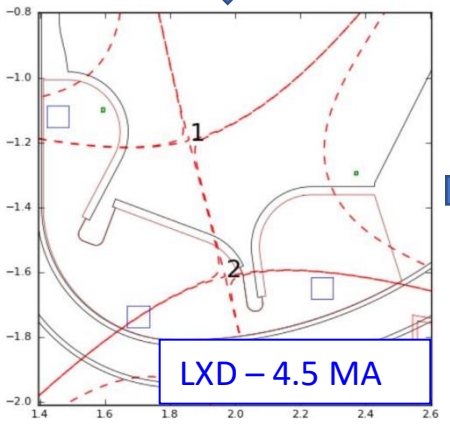

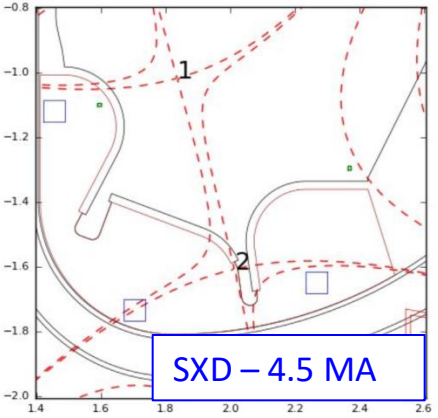

Long external leg variants

Seeding at full power

- P_{IB} = 30 MW (10 MW rad. in the inner core, 5 MW ELMs)
- P_{IB} splitted between e and D to achieve similar temperatures
- $n_{sep}=8\cdot10^{19}$ m^{-3}
- $P_{SOL}=P_{IB}-P_{rad,in}$ **(must be > 18-20 MW to access H-mode)**

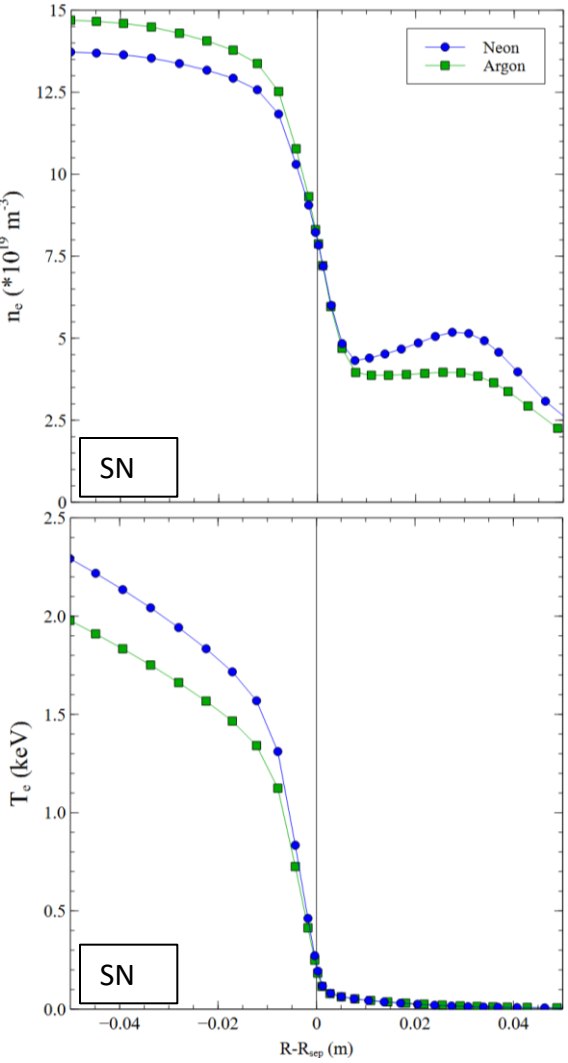

- Higher core density with argon
- Higher core temperature with neon (due to lower density)
- Higher temperature at separatrix with neon (related to Ne/Ar cooling properties)

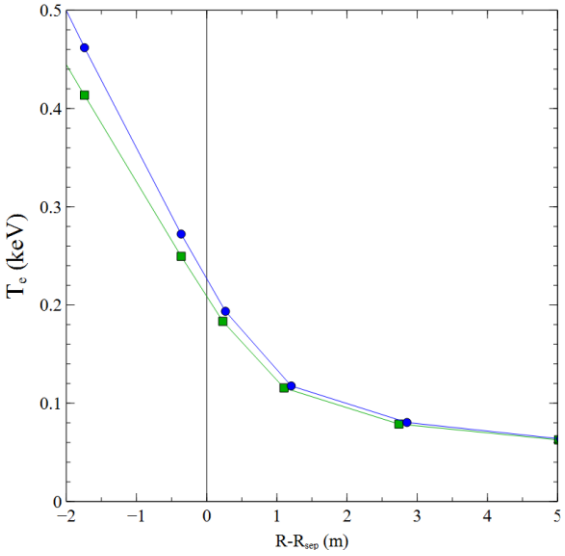

Full power seeding

Example of 2D maps for SN configuration

Neon

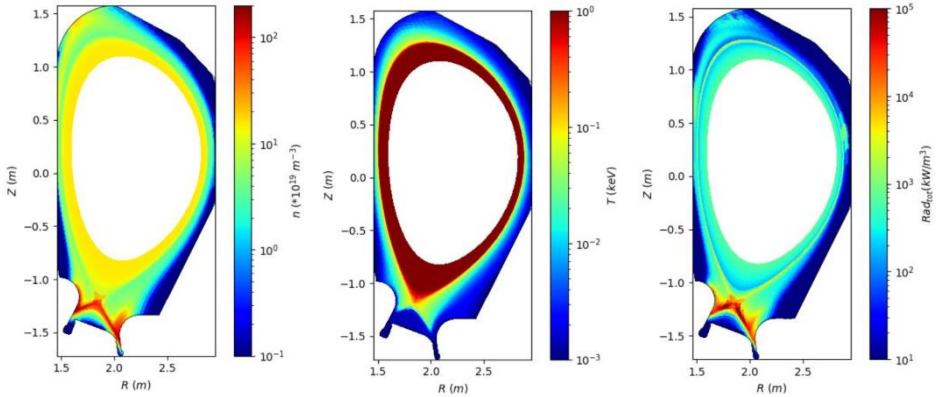

$\langle Z_{eff} \rangle_{sep}$=2.92
$P_{rad,tot}$=22.0 MW
P_{SOL}=26.0 MW
C_{imp}=2.8% **(at inner boundary)**

Radiation is concentrated on divertor legs

Argon

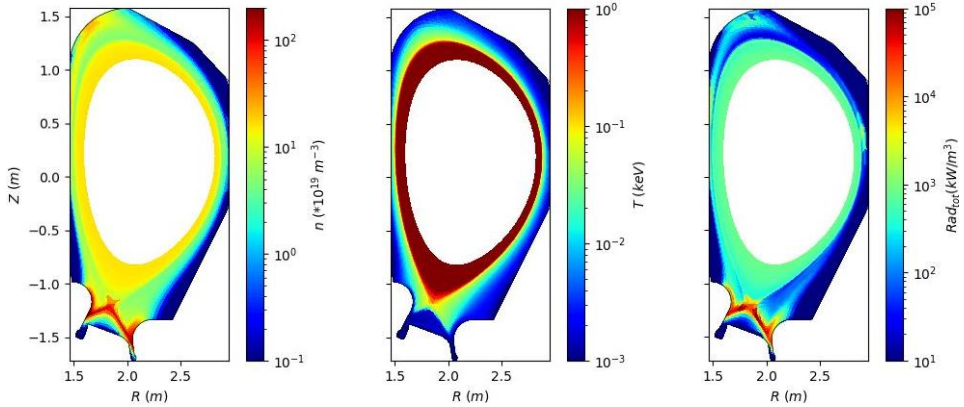

$\langle Z_{eff} \rangle_{sep}$=2.8
$P_{rad,tot}$=25.9 MW
P_{SOL}=23.7 MW
C_{imp}=1.0%

Argon provides better results than neon with similar radiation in the core

Summary of seeding results

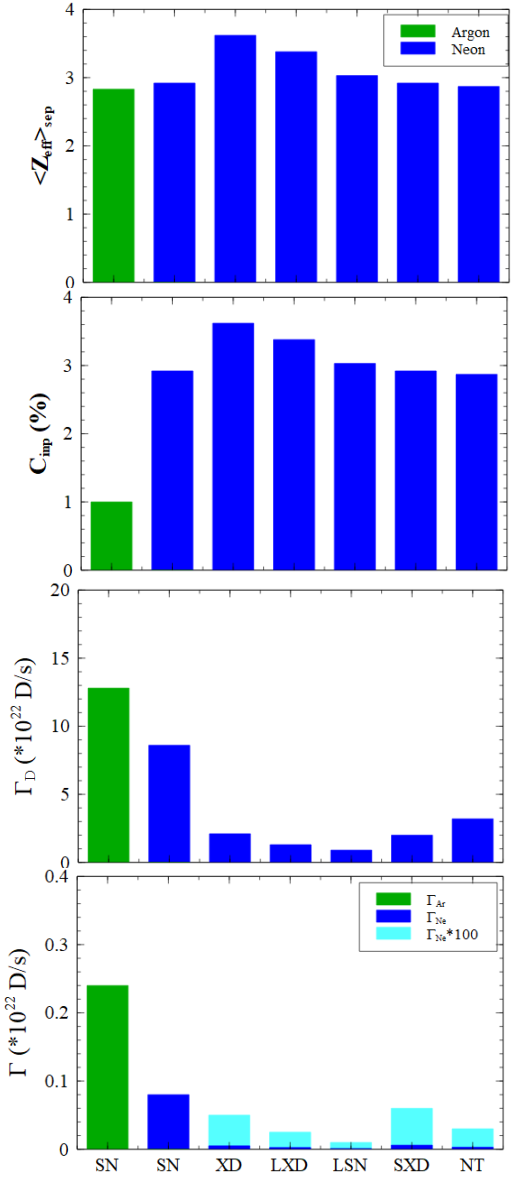

Plasma performances

Full power modeling with P_{IB}=30 MW at fixed separatrix density $n_{sep}=8\cdot10^{9}$ m^{-3} with neon (and argon) seeding to achieve detachment

- **The SN performs better than other configurations**
- Argon performs better than neon in terms of $<Z_{eff}>_{sep}$ and impurity concentration (C_{imp}) for both divertors
- **Good pumping capacity in SN for both D and seeding**
- **Low seeding pumping for other configurations**

Summary of seeding results

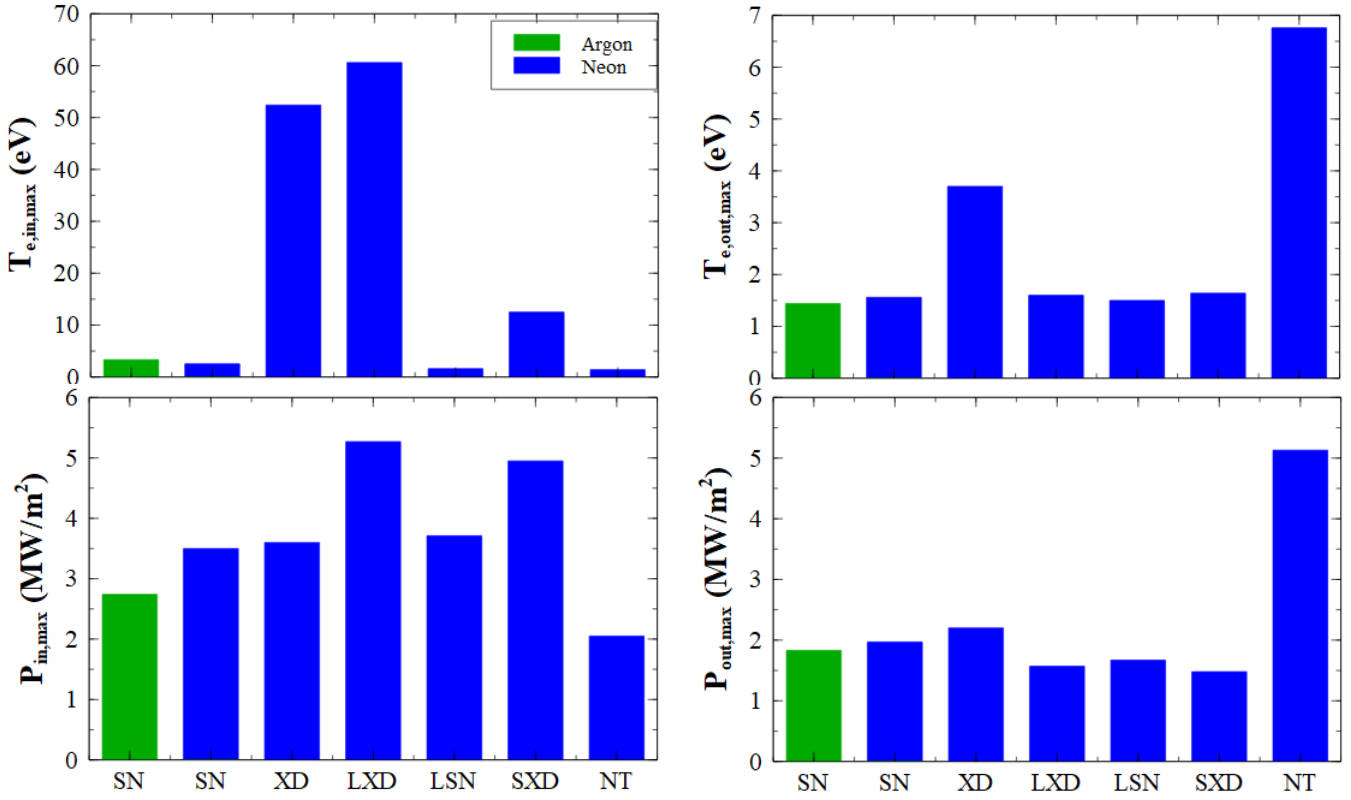

- **Detachment is difficult at the IVT for XD & LXD**
- **Detachment is difficult at OHT for NT**
- **When detached total power to the targets is well below 6 MW/m^2**

Comparison on transport and puffing position

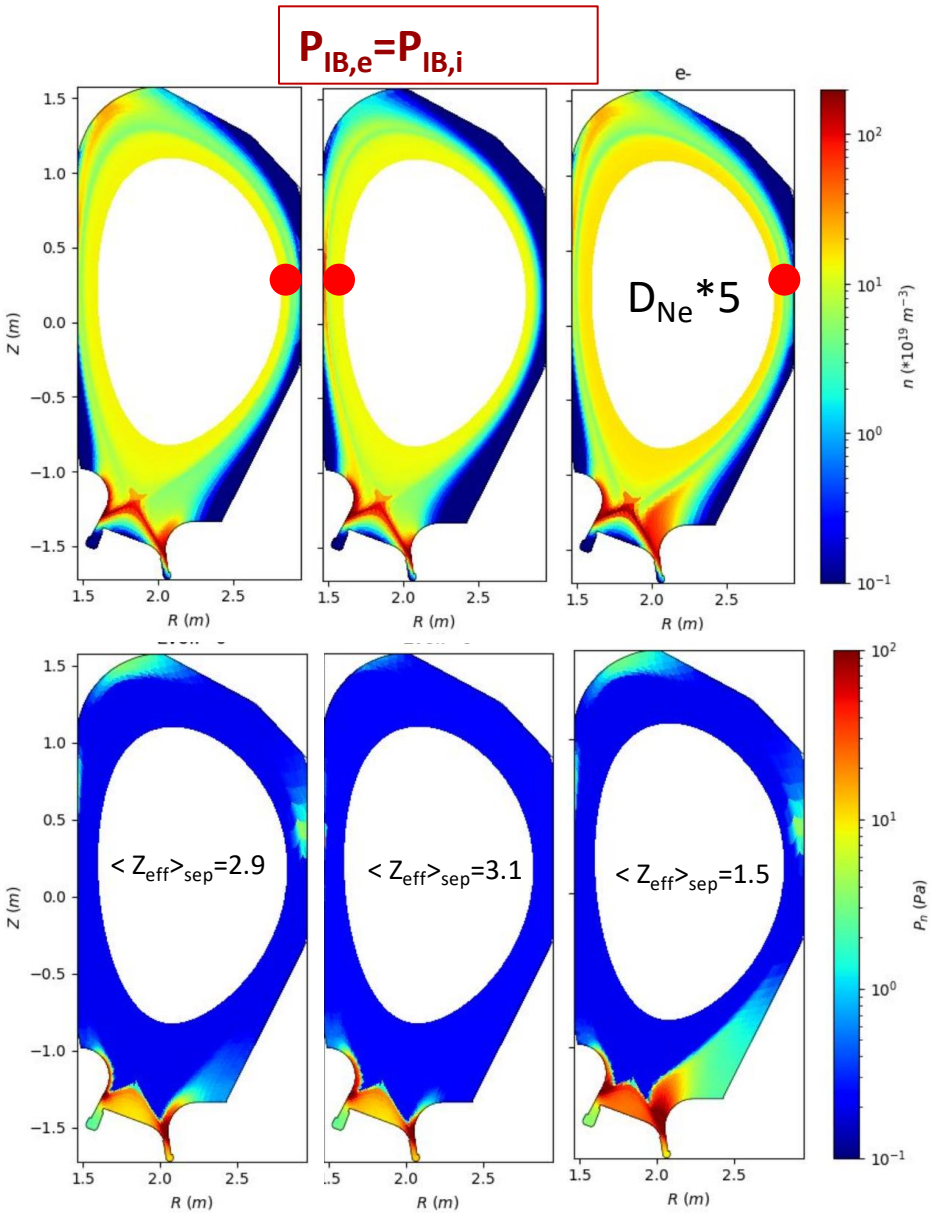

Tested different gas-puffing locations, equal P_{IB} splitting between electron and ions, higher impurity transport or lower divertor transport

- Splitting P_{in} equally between ions and electrons does not change to much the final result
- Moving gas puffing location to the high field side seems to require a higher $<Z_{eff}>_{sep}$ to achieve the same radiation level at the same separatrix density (at OMP) but the difference is well inside uncertainties
- Increasing impurity transport will reduce the required impurity content ➔ a better estimation of impurity transport is required
- Instead reducing transport in the divertor region does not change significantly the final result (not shown here)

Assessment of pumping

Assessment of pumping has been done with EIRENE including sub-divertor in modeling and setting pumps entrance a the vertical port entrance.

Sub-divertor EIRENE mesh to compute particle fluxes in a more realistic way

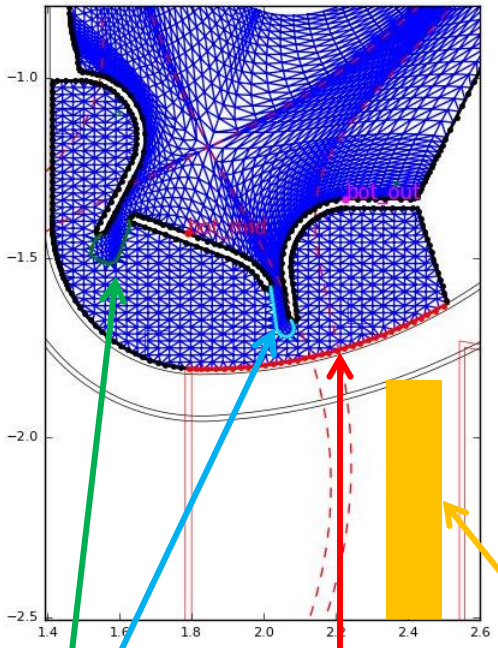

Pumps surface

Partially reflecting surfaces R=0.6

Pumps

Atomic and molecular density and pressure

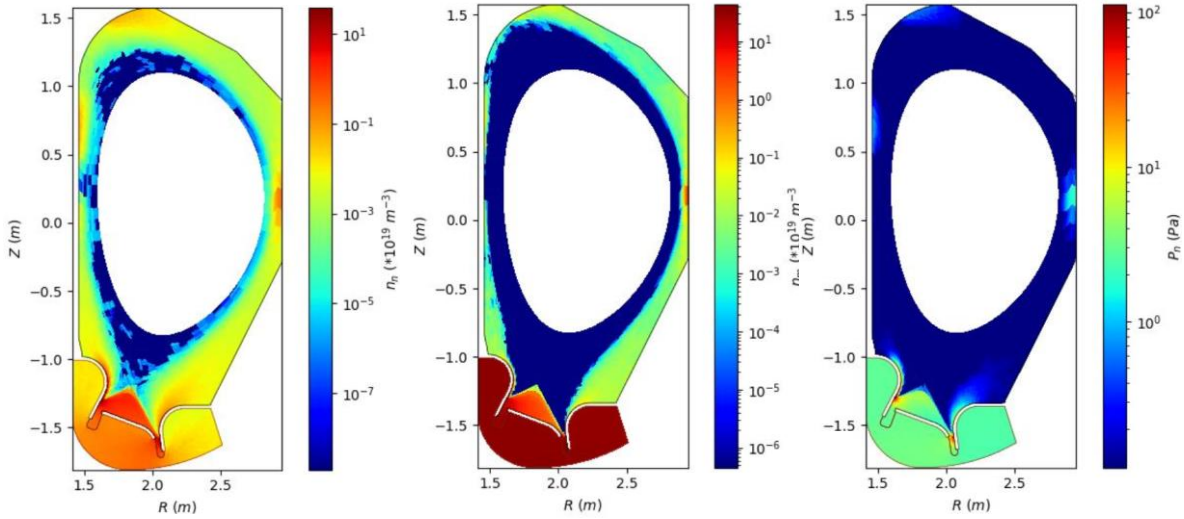

- **D Puffing Γ=5.4·10^{22} D/s**
- **Ne Puffing Γ=0.11·10^{22} Ne/s**
- Few Pa of D pressure in the sub-divertor region

* A better assessment of sub-divertor neutral dynamic by DIVGAS (C. Tantos et al 2024 Nucl. Fusion 64 016019)

XPR configuration in DTT

Objectives:

- Evaluate the possibility to operate an XPR/CRD radiative regime in the reference single null scenario
- Evaluate the range of parameters that guarantees such radiative regimes

Modelling setup:

- Transport parameters derived from scalings [1]
- P_{edge}=30MW [2]
- Fueling feedback on separatrix density ($\langle n_e \rangle_{sep}=8.0x10^{19}m^{-3}$)
- Seeding increased until XPR onset
- Neon as seeding impurity
- Multiple seeding rates tested to evaluate the XPR operative range

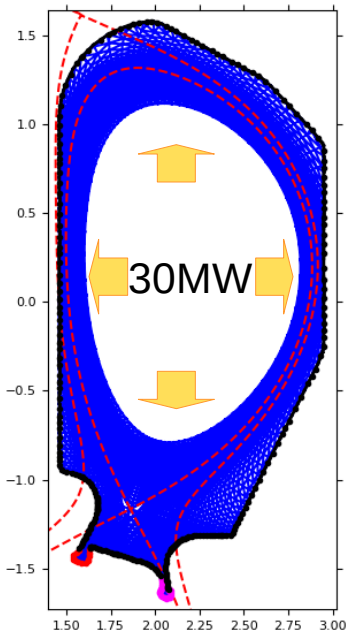

Ne seeding

SN reference scenario	
B_T [T]	6.0
I_p [MA]	5.5
R [m]	2.19
a [m]	0.7
k	1.4
q_{95}	3.0
P_{aux} [MW]	45
P_{SOL} [MW]	30
$\langle n_e \rangle_l$ m^{-3}	$20.0x10^{19}$
$\langle n_e \rangle_{sep}$ m^{-3}	$8x10^{19}$
λ_q[mm]	~1

[1] L. Balbinot et al. Nucl. Mat and Energy (2023)
[2] I- Casiraghi et al., Nucl. Fus. (2023)

XPR results

- XPR was obtained with an impurity concentration ~2%; the T_e at the X-point drops below 20eV
- The total radiation is almost constant in the seeding scan f_{rad}~90%
- A wide operative range for the XPR in terms of impurity concentration and seeding rate is observed
- XPR is lost with seeding rate <$4 \cdot 10^{20}$ Ne/s when the radiation in the confined region is below 15MW →Z_{eff}~2.0 (next slide)
- Radiative collapse is observed when seeded rate >$1.2 \cdot 10^{21}$ → Z_{eff}~2.7

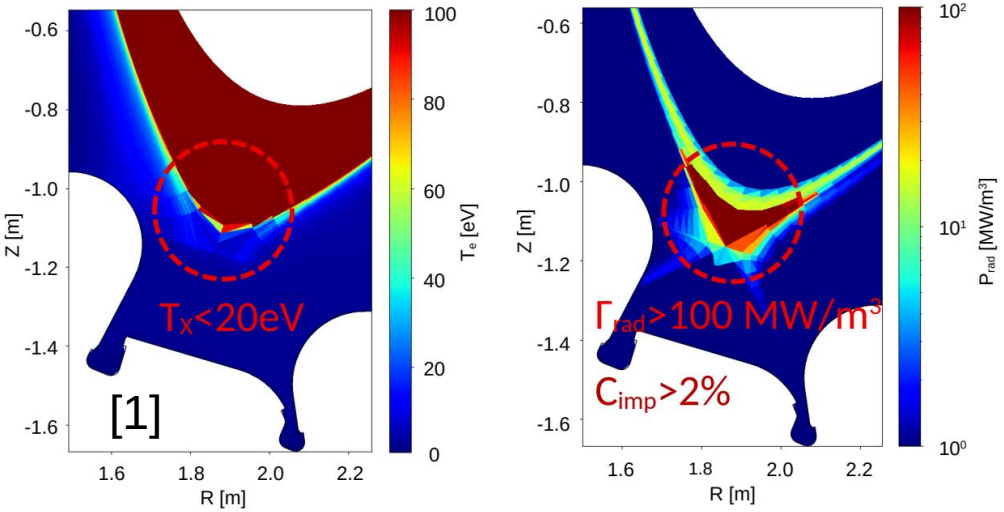

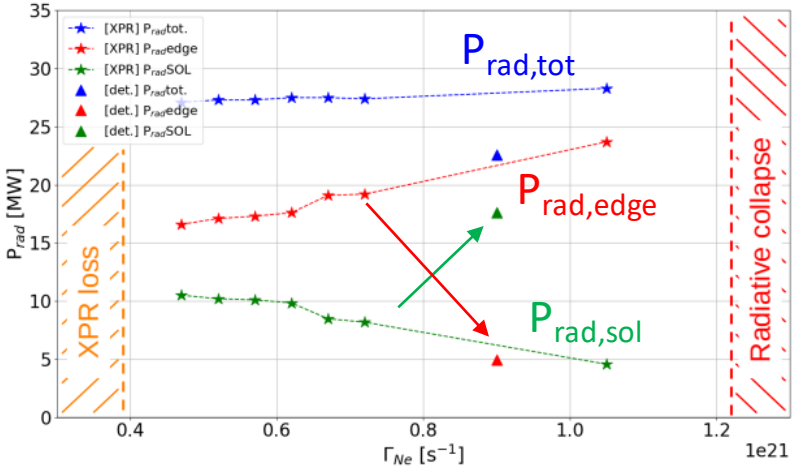

[1] L. Balbinot et al. 26th PSI 2024; to be submitted to Nucl. Mat. And Energy

XPR results

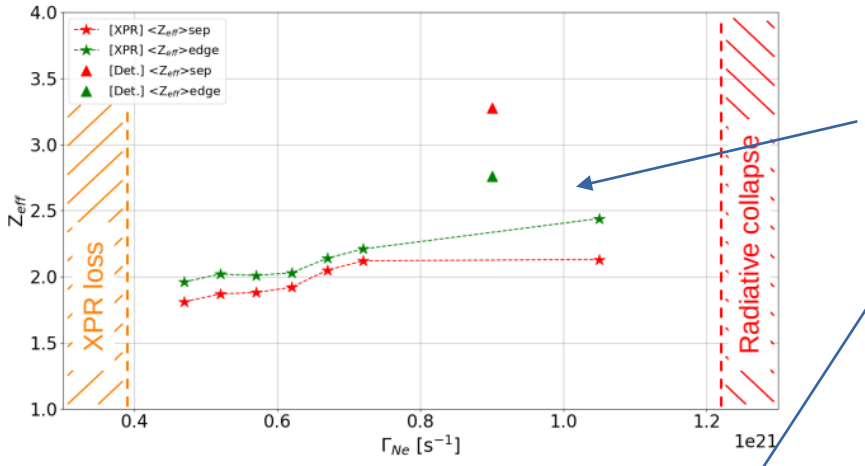

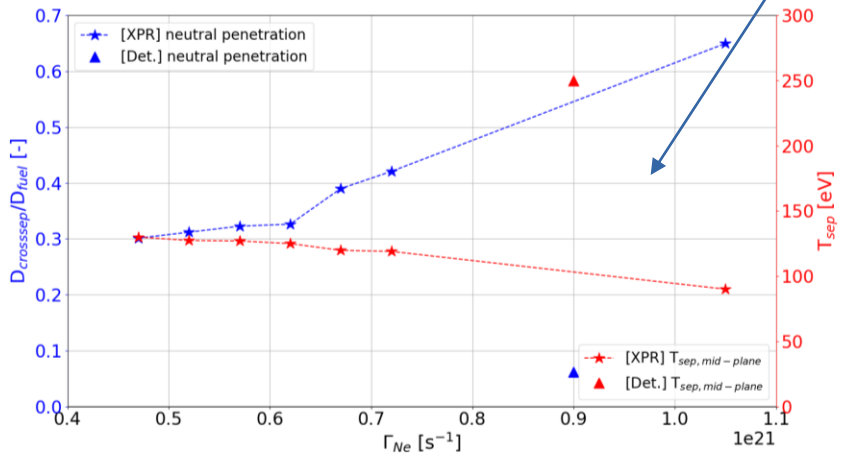

- A strong bifurcation is observed at the XPR onset
- After XPR onset, the Z_{eff} Is lower in the XPR cases (stars) than in not-XPR detached simulations (triangles)
- This is given by the extremely lower separatrix temperature of the XPR cases (half of not XPR cases) which leads to different deuterium and impurity penetration
  - Neon concentration at the pedestal top is similar between XPR and not-XPR cases
  - The large temperature difference at the XPR onset was predicted by 0D models

Ongoing modelling and analysis:

- CRD configuration was obtained with neon seeding
- The impact of $\langle n_e \rangle_{sep}$ on XPR access is being studied
- N and Ar are being tested as seeding impurities but they provide worst performances

SN: targets without/with sweeping @ PSOL=25 MW

Testing of saving divertor operation in attached plasma by sweeping

Edge modeling with very low transport parameters corresponding to $\lambda_q \approx 0.8$ mm

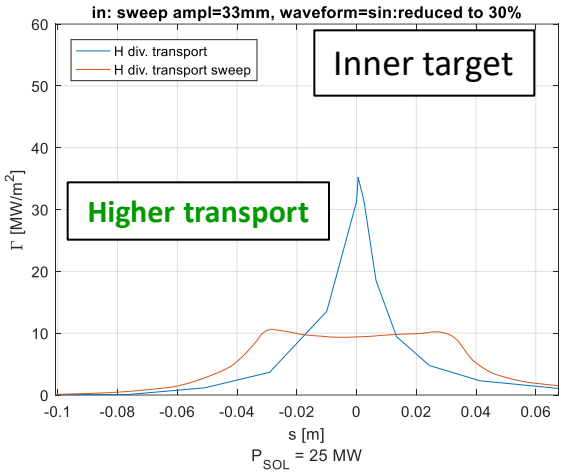

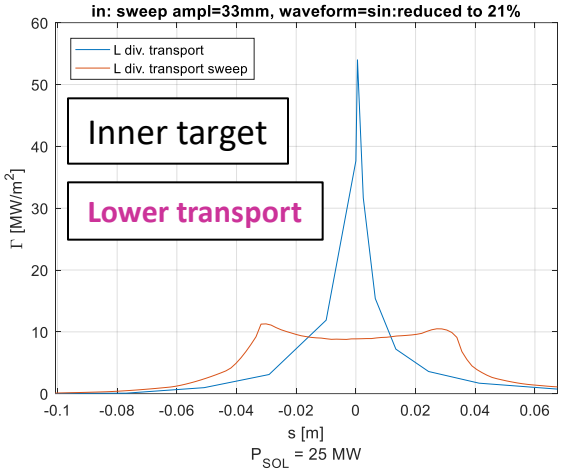

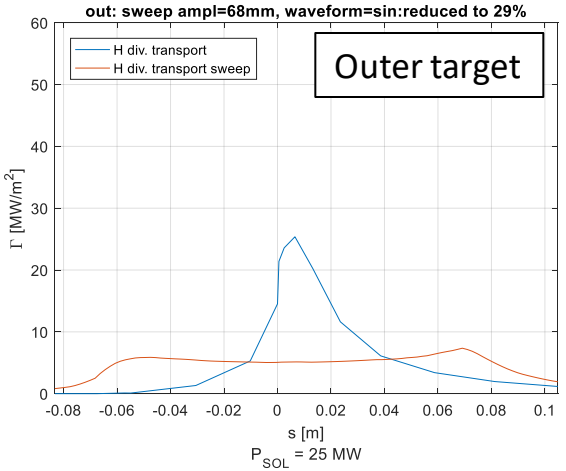

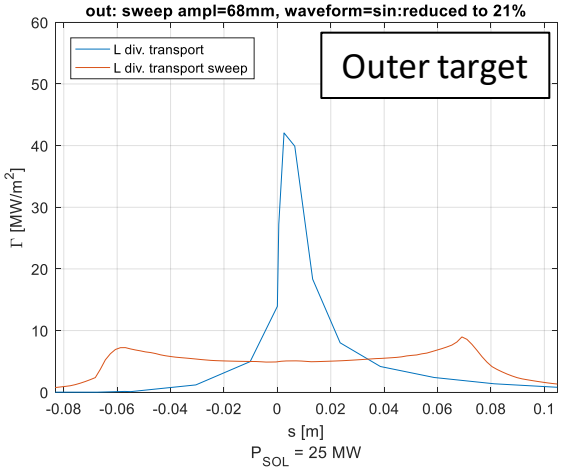

- Analyses carried out with **two different transport assumptions** so as to test the most critical conditions expected in DTT in terms:
  - **H: higher transport in the divertor region like in the far-SOL**
  - **L: lower transport in the divertor region like at the midplane**

- **Peak heat flux up to 50 MW**
- **Very narrow heat flux distribution**

In all cases heat flux reduced to/below 10 MW/m_2 with sweeping

➔ **Safe operation at very high power**

Shaping effect on the monoblock heat load

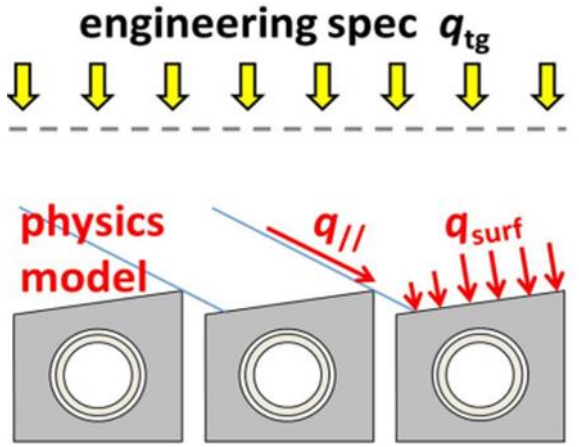

Local heat flux computed with a gyrokinetic (ion orbit) code [*] starting from 2D edge modeling to:

1. Evaluate the local temperature increase for steady state inter-ELM heat loads in both detached and attached scenarios,
2. During ELMs assuming existing scaling laws for the ELM energy fluence.

Symmetric Heat load on divertor

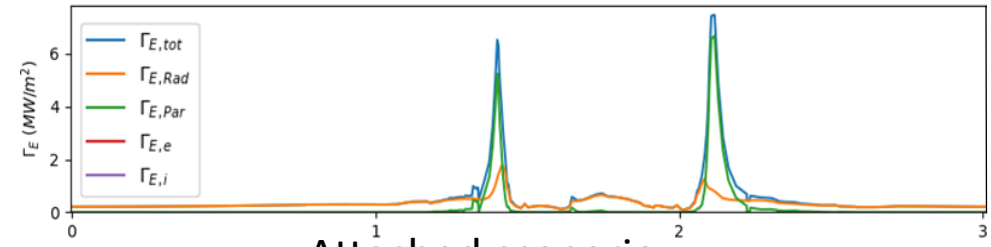

Attached scenario

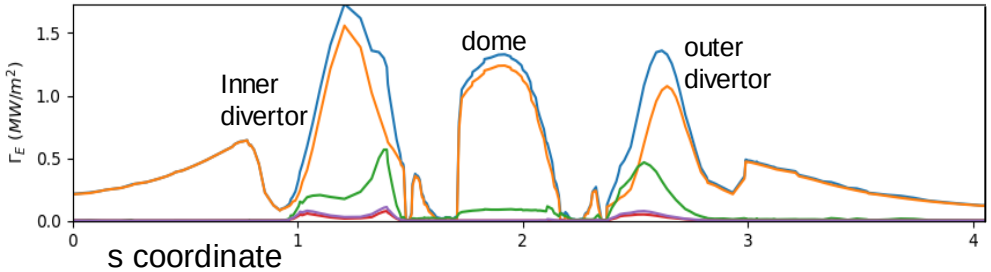

Detached inter-ELM scenario

Heat flux with:

a) Scans in radial **monoblocks misalignments**

b) Along the toroidal direction (**through the poloidal gaps**, with toroidal beveling)

c) Along the poloidal direction (**through the toroidal gaps**, without beveling).

[*] J. Gunn et al., Nucl. Fus. (2017)

Type-I ELM power and time in DTT

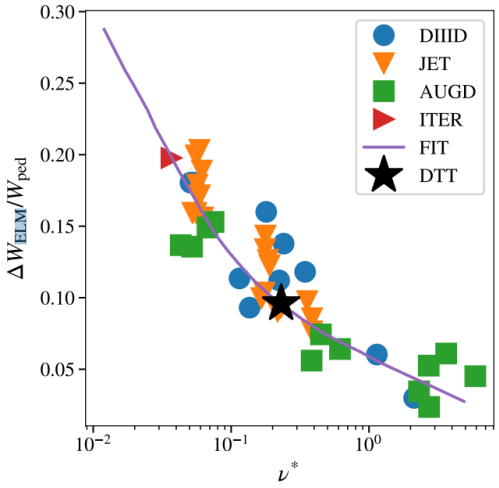

A.Loarte, *Phys Scri.* 2007
Igitkhanov, IEEE 2014

$\Delta W_{ELM} = (3\langle n_{ped}\rangle \Delta T_{ped,ELM} + 3\langle T_{ped}\rangle \Delta n_{ped,ELM}) V_{ELM}$
$W_{PED} = 3 n_{ped} T_{ped} V_{plasma}$

$\nu^* = 0.46 q_{95} R[m]/T[keV]$
$\nu^*_{DTT} = 0.23 \quad @\rho_{tor,norm} = 0.94$
$\Delta W_{ELM}/W_{PED} = 9.8\% \qquad \Delta W_{ELM} = 0.34MJ$

$\varepsilon_{//}^{peak} = 0.28 \pm 0.14 \cdot n_{e,ped}^{0.75\pm0.15} T_{e,ped}^{0.98\pm0.1} \Delta W_{ELM}^{0.52\pm0.16} R_{geo}^{1.0\pm0.4}$

$\varepsilon_{//}^{peak,DTT} = 2.10 MJ/m^2$

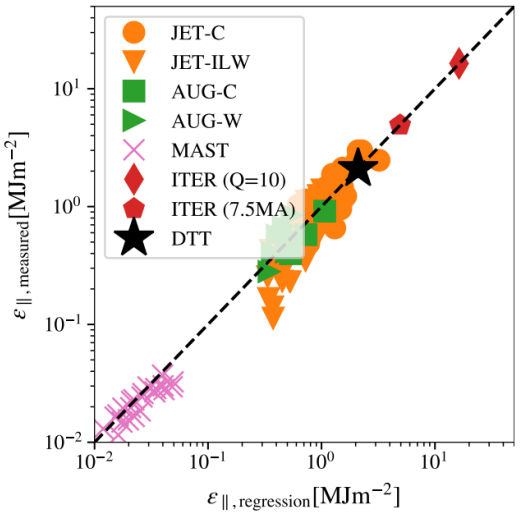

T.Eich, Nucl Mat and Energy. 2017
T. Eich, J. Nucl. Mat. 2009

According to the **free-streaming-particle model** (Fundamenski *Plasma Phys. Contr. Fus.* 2006)

- $\tau_{decay} = 2\tau_{ELM}$ (scaling τ_{ELM}~0.6 ms)
- $q_{\parallel,\mathrm{FS}}(t) = \Gamma_{\parallel,\mathrm{FS}}(t) T_e^{\mathrm{ped}} \left[\left(\frac{\tau}{t} \right)^2 + 1 \right]$
- $\Gamma_{\parallel,\mathrm{FS}}(t) = \frac{2\, n_e^{\mathrm{ped}}\, c_s^{\mathrm{ped}}}{L_\parallel / L_{\mathrm{ELM}}} \left(\frac{\tau}{t} \right)^2 \exp\left[- \left(\frac{\tau}{t} \right)^2 \right]$

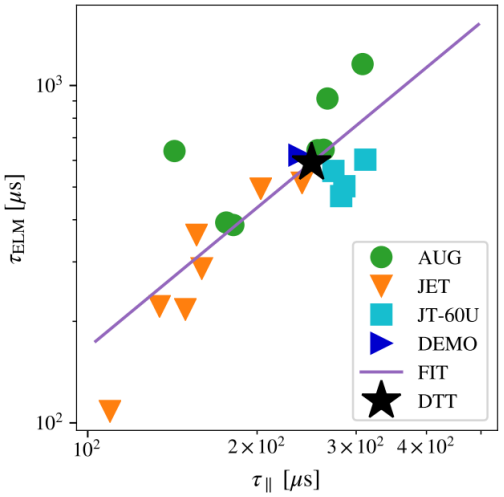

T. Eich, J. Nucl. Mat. 2009

Inter-ELM SN attached scenario

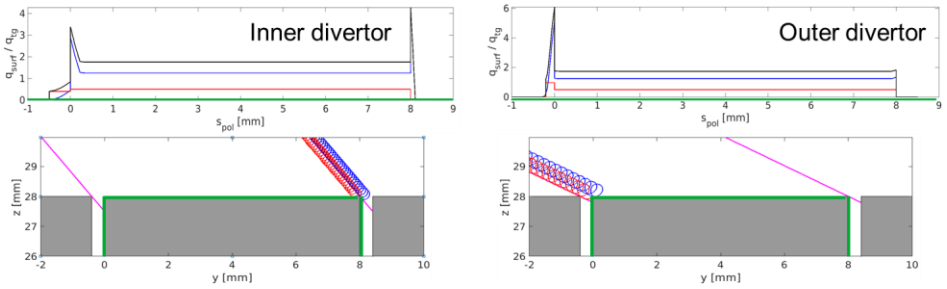

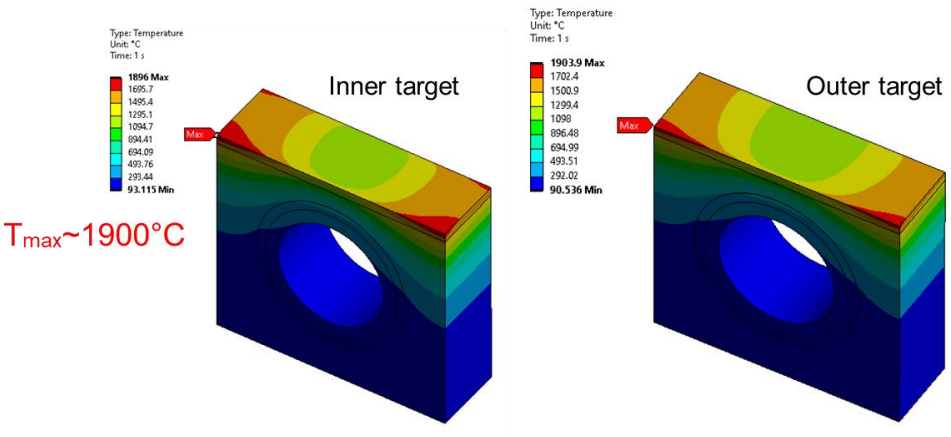

Worst case misalignments at the IVT and OVT

The **gyrokinetic effect is relevant**

- Toroidal leading edges are exposed to:
  - **6 times** higher power flux than the axisymmetric outer divertor
  - **4 times** at the inner divertor in the cases w/o radial misalignment
- The effect of **radial misalignment** is also not negligible (up to a factor 6.7 at the outer target)
- **Thermal analysis** conducted to evaluate the maximum exposure time to this kind of plasma → may became a control issue
- **Max T below W melting temperature** (3422°C), **but expected to lead to W recrystallization**

ELM response

Surface ELM energy fluence

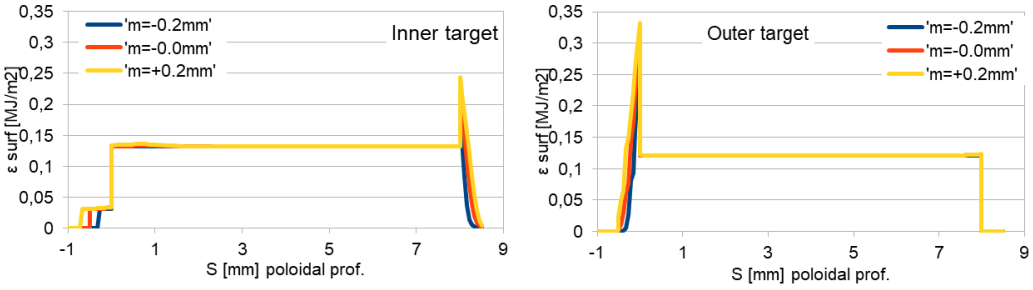

Ion orbit calculations for three values of radial misalignment

➔ The local ELM energy is dominated by ions with the peaking occurring at the lower (upper) edges of the IVT (OVT), respectively

Pfu side

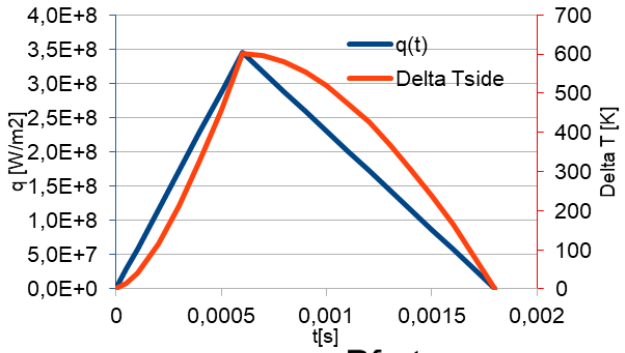

Pfu top

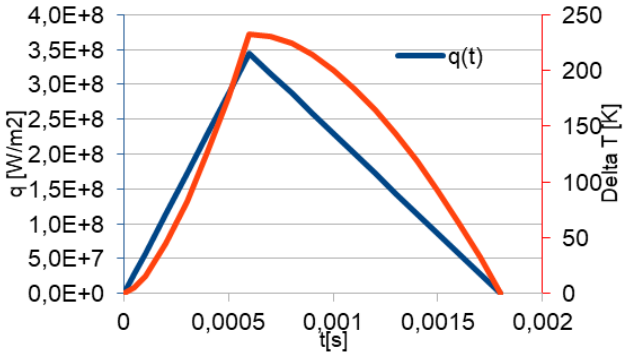

Side and top surfaces of the OVT monoblocks response to a triangular ELM waveform

The peak transient temperature of the sharp edge is given by the sum of the two curves, and yields values around 800°C for the worst case ELM.

ERO modeling

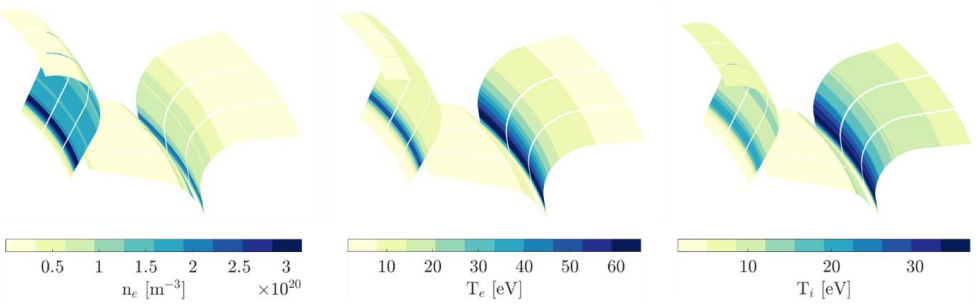

Attached plasma

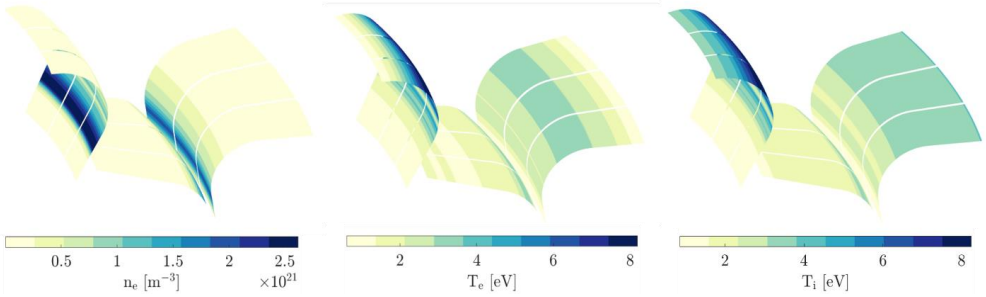

Detached plasma

Two single-null cases

1. Attached case:
   - Pure deuterium
   - P_{sol} = 14 MW
   - $n_{sep} = 7 * 10^{19}$ m^{-3}
2. Detached case:
   - Neon seeding
   - P_{sol} = 27 MW
   - $n_{sep} = 8 * 10^{19}$ m^{-3}
   - ELMs estimated from scaling

G. Alberti et al. 26th PSI 2024; to be submitted to Nucl. Mat. And Energy

ERO results: erosion in ELMs free

INNER TARGET

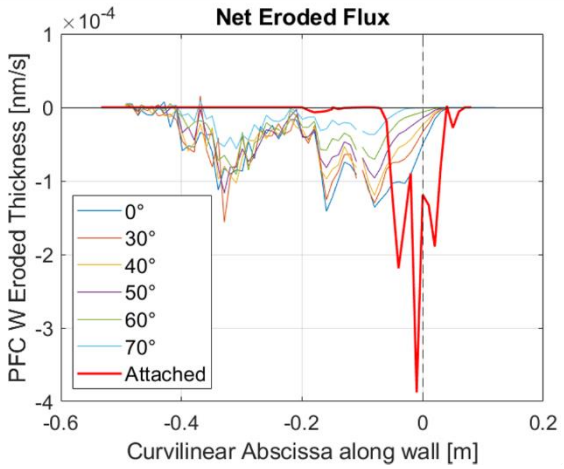

DOME

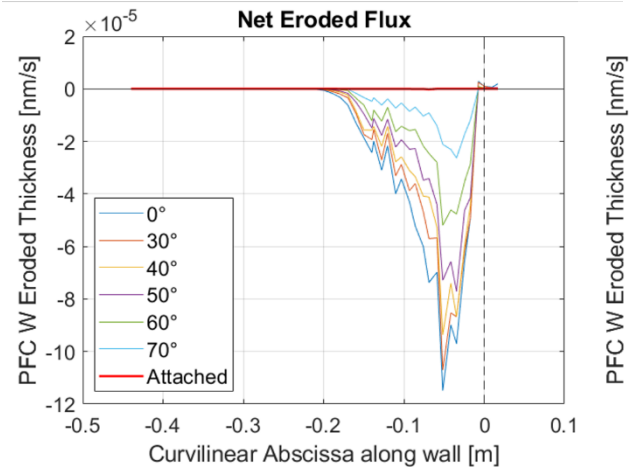

OUTER TARGET

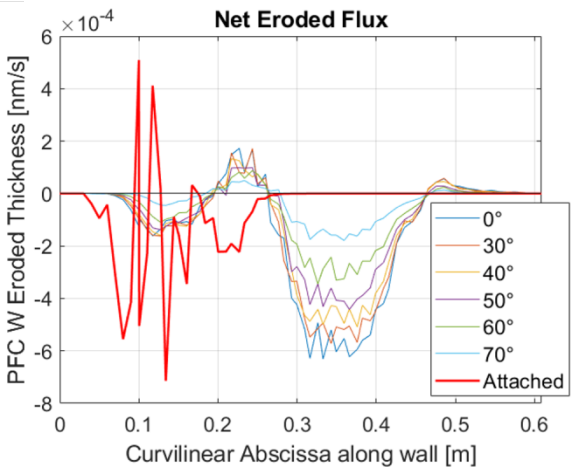

No W deposition from first wall considered

- No clear erosion dependence on D incidence angle for attached case ➔ 1 case shown
- Strong dependence on incidence angle for Ne ions ➔ scan presented

Similar erosion for attached and detached:

- In attached **due to D at high temperature**
- In detached **due to Ne ions** (up to 10+ ionization state)

W screaning

INNER TARGET

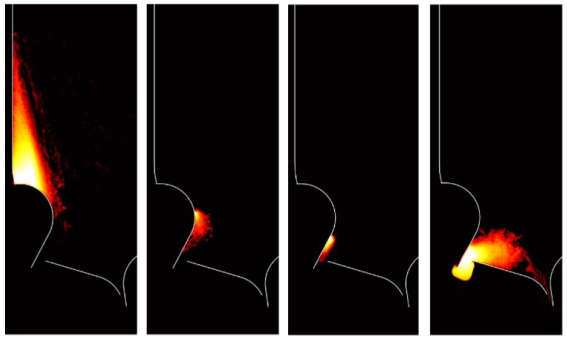

DOME

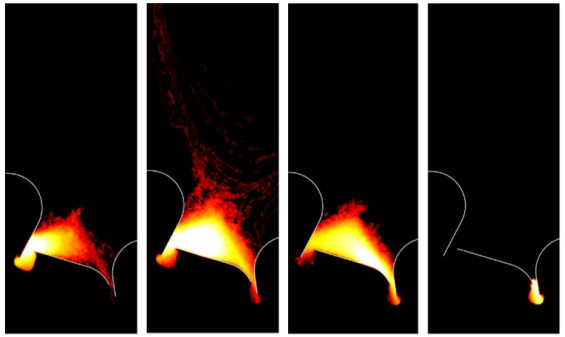

OUTER TARGET

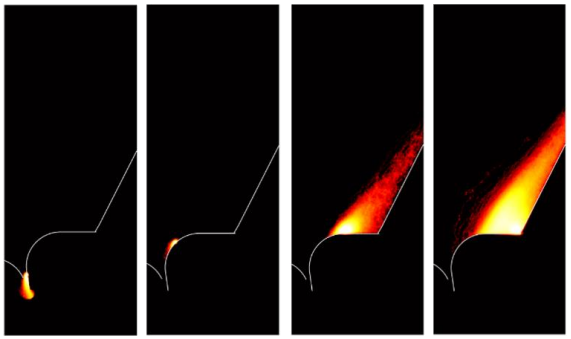

W source scan is detached plasma

- ❖ Same W source in different positions on the divertor.

- ➢ **Good screening at the inner ad outer target** (due to high density)
- ➢ Relatively good screening at the sides of flat dome
- ➢ Poor screening at the central part of dome and top of inner/outer targets (low density in front)

ERO results: erosion intra ELMs

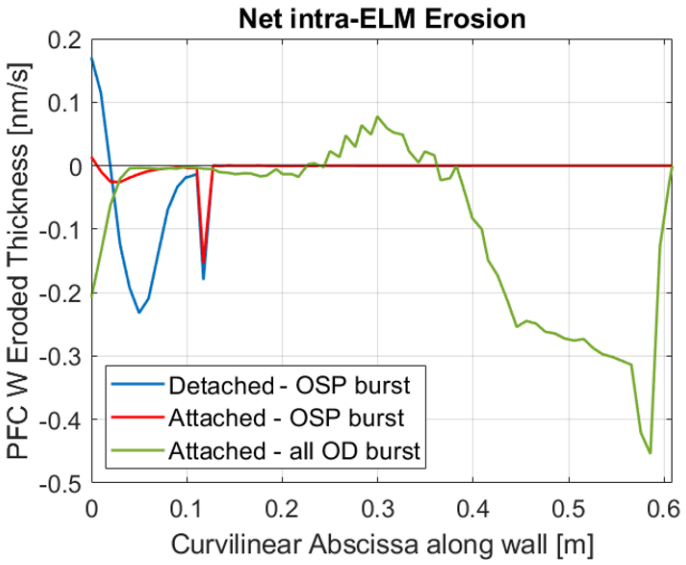

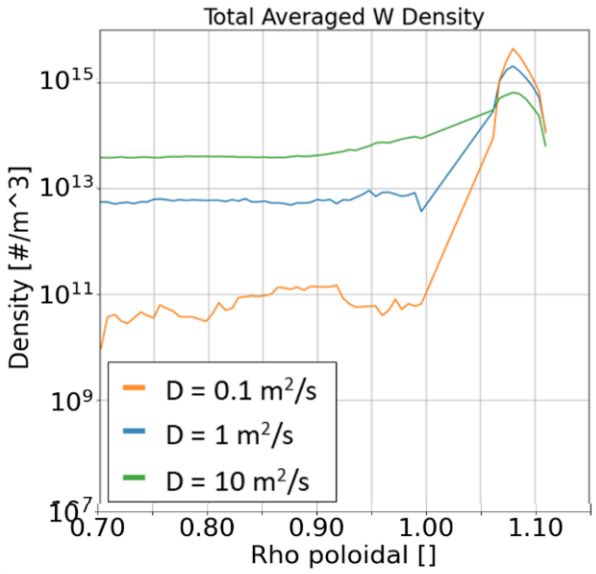

Considered burst of D^+ ions at the pedestal top temperature of 1 keV (***ΔW_{ELM}=0.34 MJ***)

1. OD burst: extended onto the whole outer divertor (all).
2. OSP burst: energetic D+ ions concentrated only on the entire outer vertical target
   - In OD Very high erosion in the far target due to poor screening
   - Lower net erosion due to higher prompt redeposition in attached case

- W density into the core **below acceptable limits** even in this extreme case anomalous cross-field diffusion coefficients
- In general, **prompt redeposition tends to be higher in attached case**, due to the higher temperatures near divertor surface.

ELMs modelling based on assumptions from Kirschner A. et al, NME 18 (2019) 239244

Conclusions

- The DTT divertor has been designed to be able to accept many magnetic configuration at high power using all its sub-sections (IVT, CHT,OVT,OHT)
- Edge modeling of DTT reference magnetic configurations have been done at full power with realistic transport profiles to optimized the divertor shape
- The resulting divertor is optimized for the SN-PT configuration but the others can provide similar performance in term of power exhaust capability
- Although divertor optimization was not based on XPR configuration, modeling has shown that it can be accessed with good performances
- Pumping capability has been estimated including sub-divertor region in edge modeling and with dedicated neutrals kinetic code
- Strike points sweeping has been evaluated and considered as a way avoid tungsten melting in case of accidental attachment
- The effect of monoclocks shaping has be evaluated by an ion orbit code and also considering ELMs
- Tungsten erosion and diffusion in plasma core has been studied with ERO code in attached/detached and during ELMs. Preliminary results seems to indicate a low core contamination